

Seed banks can help to maintain the diversity of interacting phytoplankton species

Coralie Picoche^{1,2,*} & Frédéric Barraquand^{1,2}

¹Institute of Mathematics of Bordeaux, University of Bordeaux and CNRS, Talence, France

²Integrative and Theoretical Ecology, LabEx COTE, University of Bordeaux, Pessac, France

Abstract

Seed formation is part of the reproductive cycle, leading to the accumulation of resistance stages that can withstand harsh environmental conditions for long periods of time. At the community level, multiple species with such long-lasting life stages can be more likely to coexist. While the implications of this process for biodiversity have been studied in terrestrial plants, seed banks are usually neglected in phytoplankton multispecies dynamic models, in spite of widespread empirical evidence for such seed (or rather cyst) banks. In this study, we build a metacommunity model of interacting phytoplankton species with a cyst bank. The model is parameterized with empirically-driven growth rate functions and field-based interaction estimates, which include both facilitative and competitive interactions. Exchanges between compartments (coastal pelagic cells, coastal cysts on the seabed, and open ocean pelagic cells) are controlled by hydrodynamical parameters to which the sensitivity of the model is assessed. We consider two models, i.e., with and without a saturating effect of the interactions on the growth rates. Our results are consistent between models, and show that a cyst bank allows to maintain all species in the community over 30 years. Indeed, a fraction of the species are vulnerable to extinction at specific times within the year, but this process is buffered by their survival in the coastal cyst bank. We thus highlight the potential role of the cyst bank in the recurrent re-invasion of the coastal community, and of coastal environments in re-seeding oceanic regions. Moreover, the cyst bank enables populations to tolerate stronger interactions within the community as well as more severe changes in the environment, such as those predicted within a climate change context. Our study therefore shows how a cyst stage may help phytoplanktonic diversity maintenance.

Keywords: phytoplankton; seed bank; dormancy; cyst; coexistence; facilitation

*corresponding author: coralie.picoche@u-bordeaux.fr

Introduction

How the high biodiversity of primary producers maintains is still an unresolved question for both experimental and theoretical ecology. Terrestrial plants and phytoplanktonic communities can present hundreds of species relying on similar resources, a situation where Gause's principle implies that a handful of species should outcompete the others. Some degree of niche differentiation, perhaps hidden to the human observer, is generally expected for coexistence to maintain (Chesson, 2000). However, a complex life-history structure can further increase the likelihood of coexistence (e.g. Moll & Brown, 2008; Fujiwara *et al.*, 2011), and so does the response of life history traits to variation in the environment (Chesson & Huntly, 1988; Huang *et al.*, 2016).

Analyses of coexistence in terrestrial plant communities sometimes take into account several life stages (e.g., Aikio *et al.*, 2002; Comita *et al.*, 2010; Chu & Adler, 2015) though many consider only a single life-stage (see, among others, Ellner, 1987; Levine & Rees, 2004; Martorell & Freckleton, 2014). When considering at least two stages, seeds/seedlings and adults, several mechanisms that can contribute to long-term coexistence in spatially and/or temporally fluctuating environment have been uncovered (Shmida & Ellner, 1984; Chu & Adler, 2015). The storage effect, a major paradigm in modern coexistence theory (Chesson, 2000, 2018) which involves covariances between competitive strengths and environmental variation, is one of them. It has been shown to arise when a long-lived dormant stage combines with temporal variation in recruitment from this stage and interspecific competition (Cáceres, 1997) and is often discussed in connection to seed banks (Aikio *et al.*, 2002; Angert *et al.*, 2009). However, the contribution of seeds to coexistence may be much larger than their potential contribution to the storage effect. A long-lived seed bank can help coexistence by other, simpler means. For instance, in the meta-community model of Wisnoski *et al.* (2019), when dormancy and dispersal are present (without seed dispersal), local diversity increases in temporally fluctuating environments. In their model, adding a dormant stage could increase species diversity both at the local and regional scales. These results suggest that considering a seed stage in

dynamical models can profoundly alter our understanding of community persistence (see also Jabot & Pottier, 2017).

Although there is some awareness of the role of cryptic life stages in shaping terrestrial plant coexistence, the effect of such dormant life stages on aquatic plant communities, and more specifically that of phytoplanktonic algae, is often ignored. The classical view behind phytoplankton dynamics is that their blooms (peaks in abundances several orders of magnitude above their baseline level) are due to seasonal variation in light, temperature and nutrients, as well as hydrodynamic processes (Reynolds, 2006). In this mindset, differential responses to environmental signals ensure the coexistence of multiple species (Margalef, 1978; Smayda & Reynolds, 2001), while always assuming that vegetative cells are already present in the environment, or immigrating from a nearby water mass. Momentary disappearances of a species are viewed as sampling issues at low density. However, a complementary hypothesis suggests that resuspension and germination of phytoplanktonic resting cells, or cysts, is another major player allowing re-invasion from very low or locally zero population densities (Patrick, 1948; Marcus & Boero, 1998). This long-standing hypothesis is supported by recent reviews (Azanza *et al.*, 2018; Ellegaard & Ribeiro, 2018) which confirm that life history strategies including dormant cysts are widespread in phytoplankton. Cyst formation can either be part of the life cycle of phytoplankton species and result from sexual reproduction or be triggered by specific environmental conditions, leading to asexual resting stages (Ellegaard & Ribeiro, 2018). A variety of models have endeavoured to explain and predict amplitude, timing and/or spatial distribution of blooms by explicitly modeling multiple stages in the life cycle of a particular species, but without interactions with other organisms (see for example McGillicuddy *et al.*, 2005; Hense & Beckmann, 2006; Hellweger *et al.*, 2008; Yñíguez *et al.*, 2012). Two-to-four species (Yamamoto *et al.*, 2002; Estrada *et al.*, 2010; Lee *et al.*, 2018) models also exist, but they focus on explaining the dynamics of a single cyst-forming species or group interacting mostly with vegetative-only groups. This state of affairs means that we currently have no clear understanding of how the cyst stage might help maintain biodiversity

in species-rich communities. In the present paper, we demonstrate the potential role of cyst banks using a phytoplankton community dynamics model including a cyst bank.

Phytoplankton communities in coastal environments may benefit from seed banks (hereafter called cyst banks to be more consistent with the terminology in use for such species) even more than the oceanic communities (see for example McGillicuddy *et al.*, 2005), as the distance to the sea bottom is smaller, which favours recolonization from the sea bottom, something that is impossible in the deep ocean. Moreover, ‘horizontal’ exchanges between oceanic and coastal pelagic phytoplanktonic communities are usually observed. A flow from the ocean to coastal communities has been noticed for dinoflagellates especially (Tester & Steidinger, 1997; Batifoulier *et al.*, 2013). Conversely, in many other bloom-forming species, the shallower coastal areas might function as a reservoir for biodiversity in the ocean. Indeed, cysts are able to germinate again after dozens of years (McQuoid *et al.*, 2002; Ellegaard & Ribeiro, 2018) or even thousands of years (Sanyal *et al.*, 2018) of dormancy. Therefore, we consider in this study three interlinked compartments: the coastal pelagic environment, the cyst bank, and the pelagic open ocean. The coastal pelagic environment acts as a bridge between the cyst bank and the open ocean.

Our model is parameterized from field data (growth and interaction rates), and includes biotic and abiotic constraints (e.g., particle sinking). In our analyses, we examine how cyst banks may influence the maintenance of biodiversity, including under changing biotic interactions or changing environmental conditions. We either add or remove the dormant compartment, which allows to pinpoint its contribution to coexistence. We find that the presence of cysts prevents the extinction of several species. Cyst banks also allow a community to maintain its richness even with strong disturbances of its interaction network, unless facilitative interactions completely eclipse competitive interactions. Changes in the environment, here represented by an increase in the mean temperature, can also be buffered by cyst banks. Finally, we discuss what information would be required to further more accurate modeling of cyst bank dynamics.

Methods

Models

Our models (Fig. 1) build atop recent models developed by Shoemaker & Melbourne (2016) and Wisnoski *et al.* (2019), although they diverge in several aspects developed below (e.g., possibility for facilitative interactions). These discrete-time models are designed for meta-communities with multiple interacting populations. Any discrete-time model requires an ordering of events; in our models, these unfold as follows: first, populations grow or decline according to a Beverton-Holt (BH) multispecies density-dependence (eqs. 1 and 3), and then, in a second step, exchanges occur between the different compartments or patches constituting the metacommunity (eq. 4).

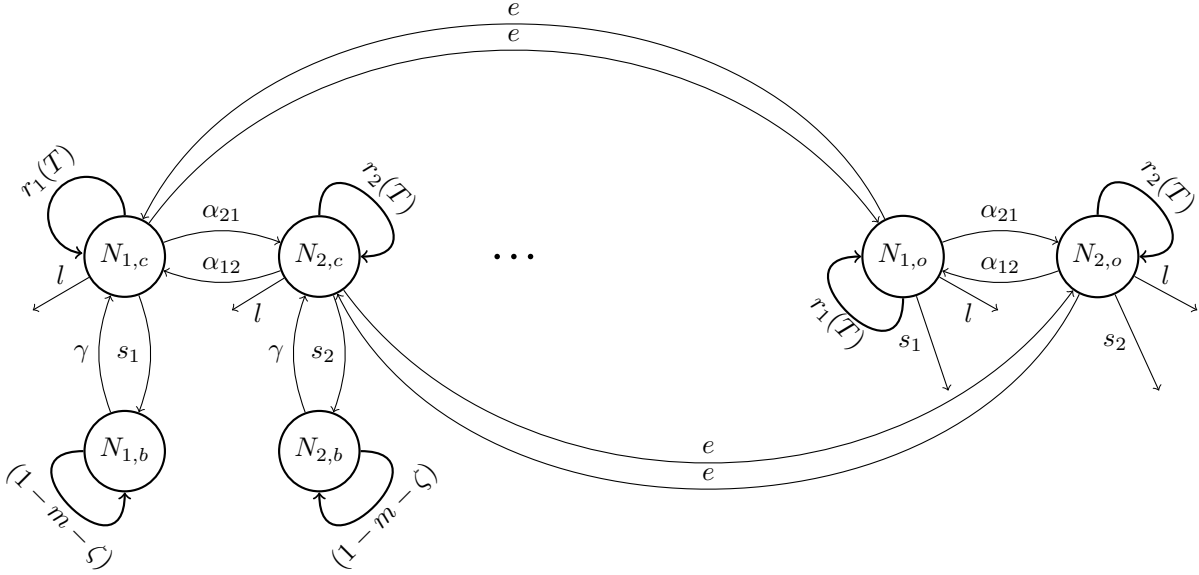


Figure 1: Structure of the model. Phytoplanktonic species (represented by circles) are present in the coast (subscript c), the ocean (o) and the cyst bank (b). Parameters governing demography, interactions between organisms and exchanges between compartments are defined in Table 1. Only two species are shown here for the sake of simplicity but 11 species are present in the model.

In this paper, individuals are phytoplanktonic cells that move between the upper layer of coastal water, its bottom layer where a cyst bank accumulates in the sediment, and the

oceanic zone surrounding the coastal water masses (hereafter “the ocean”). Only oceanic and coastal pelagic cells are subject to BH-density dependence. Cysts are only affected by mortality m and burial due to sedimentation ζ . Parameters and state variables are defined in Table 1.

The Beverton-Holt (BH) formulation of multispecies population dynamics, sometimes called Leslie-Gower (Cushing *et al.*, 2004), is a Lotka-Volterra competition equivalent for discrete-time models, and is often used to represent terrestrial plant community dynamics. In our implementation of the model, the maximum achievable growth rate is modified by both competitive and facilitative interactions, which translates into positive and negative α_{ij} coefficients, respectively. We present two different interaction models. We first use the classical multispecies BH model (model I, eq. 1), also present in the original models of Shoemaker & Melbourne (2016) and Wisnoski *et al.* (2019). However, the high number of facilitative interactions characterizing the modeled phytoplankton community (Picoche & Barraquand, 2020) combined to the mass-action assumption could have very unrealistic destabilizing consequences, which have been likened to an “orgy of mutual benefaction” (May, 1981): populations grow to infinity because there is no saturation of beneficial effects when density increases. In model I, we therefore forbid the realized growth rate to go above the intrinsic growth rate (its theoretical limit), by setting a minimum value of 1 to the denominator of the BH formulation. We subsequently define saturating interactions, inspired by Qian & Akçay (2020), in our model II (eq. 3). Model II provides a more process-orientated solution to the issue of excessive mutual benefaction (but at the cost of added parameters).

In our framework, the first step of model I can be written as

$$\begin{cases} N_{t',i,c} &= \frac{\exp(r_i(T))N_{t,i,c}}{1+\sum_j \alpha_{ij}N_{t,j,c}} - lN_{t,i,c} \\ N_{t',i,o} &= \frac{\exp(r_i(T))N_{t,i,o}}{1+\sum_j \alpha_{ij}N_{t,j,o}} - lN_{t,i,o} \\ N_{t',i,b} &= N_{t,i,b}(1 - m - \zeta) \end{cases} \quad (1)$$

where the intrinsic growth rate $r_i(T)$ is a species-specific function of the temperature (see eq.

2), the interaction coefficients α_{ij} are per capita effects of species j on species i , and the loss term l accounts for lethal processes such as natural mortality, predation or parasitism. First estimates of interaction coefficients are inferred from a previous study of coastal community dynamics with Multivariate AutoRegressive (MAR) models (Picoche & Barraquand, 2020). We later calibrate these coefficients for model I, since MAR models were applied at a different timescale.

The intrinsic growth rate $r_i(T)$ is defined through a modified version of the formula used by Scranton & Vasseur (2016) (eq. 2), which classically decomposes $r_i(T)$ in two parts: the species-independent metabolism part $E(T)$ and the species-specific niche part $f_i(T)$:

$$\begin{aligned}
 r_i(T) &= E(T)f_i(T) \\
 \text{where } E(T) &= d \times 0.81e^{0.0631(T-273.15)} \\
 \text{and } f_i(T) &= \begin{cases} \exp(-|T - T_i^{opt}|^3/b_i), & T \leq T_i^{opt} \\ \exp(-5|T - T_i^{opt}|^3/b_i), & T > T_i^{opt}. \end{cases}
 \end{aligned} \tag{2}$$

The metabolism part describes the maximum achievable intrinsic growth rate based on Bissinger *et al.* (2008). This maximum daily intrinsic growth rate is weighted by the daylength d as no growth occurs at night. The niche part $f_i(T)$ describes the decrease in growth rate due to the difference between the temperature in the environment and the species-specific thermal optimum T_i^{opt} , and is controlled by the species-specific thermal decay b_i , which depends on the niche width. Parameterisation is further detailed in Section S1 of the SI.

In model II, oceanic and coastal dynamics are governed by eq. 3.

$$N_{t',i,c/o} = \frac{\exp(r_i(T))N_{t,i,c/o}}{1 + \sum_{j \in \mathbb{C}} \frac{a_C N_{t,j,c/o}}{H_{ij} + N_{t,j,c/o}} + \sum_{j \in \mathbb{F}} \frac{a_F N_{t,j,c/o}}{H_{ij} + N_{t,j,c/o}}} - lN_{t,i,c/o} \tag{3}$$

where a_C and a_F are the maximum competition and facilitation strengths, respectively, with

\mathbb{C} and \mathbb{F} the sets of competitors and facilitators of species i . We use here similar notations to Qian & Akçay (2020), but use different parameters that vary between species. Indeed, the half-saturation coefficients H_{ij} vary between species, as opposed to the maximum rates in Qian & Akçay (2020). It did not make sense biologically for H_{ij} to be fixed (e.g., in a resource competition context, different species are expected to feel resource limitations at different concentrations of nutrients and at different numbers of competitors). How to shift from MAR- to BH-interaction matrices in model I, and to use the parameter estimates of model I to specify parameters in model II is described in Section S2 of the SI.

After growth and mortality processes occur, exchanges take place between the three compartments, which constitutes the second step of the model (eq. 4):

$$\begin{cases} N_{t+1,i,c} &= (1 - s_i - e)N_{t',i,c} + \gamma N_{t',i,b} + eN_{t',i,o} \\ N_{t+1,i,o} &= (1 - s_i - e)N_{t',i,o} + eN_{t',i,c} \\ N_{t+1,i,b} &= (1 - \gamma)N_{t',i,b} + s_i N_{t',i,c} \end{cases} \quad (4)$$

Parameter	Name	Value (unit)	Status
$N_{t,i,c/o/b}$	Abundance of species i at time t in the coast (c), ocean (o), or coastal bank (b)	NA (Number of cells)	Dynamic
T	Temperature	NA (K)	Dynamic
$r_i(T)$	Intrinsic growth rate of species i	NA (day^{-1})	Dynamic
b_i	Thermal decay	Field-based (K^3)	Calibrated
T_i^{opt}	Optimal temperature for species i	Field-based (K)	Calibrated
d	Daylength	50 (%)	Fixed
α_{ij}	Interaction strength of species j on i in model I	Field-based (Cells^{-1})	Calibrated
a_C/a_F	Maximum competitive/facilitative interaction strength in model II	Field-based (NA)	Calibrated
H_{ij}	Half-saturation for the interaction strength of species j on i in model II	Field-based (Cells)	Calibrated
s_i	Sinking rate of species i 's cyst	$\{0.1; \mathbf{0.3}; 0.5\} \times \beta(0.55, 1.25)$ (day^{-1})	Fixed
e	Exchange rate between ocean and coast	$\{0; \mathbf{0.4}; 0.9\}$ (day^{-1})	Fixed
l	Loss rate of pelagic phytoplanktonic cells	$\{0.04; 0.1; \mathbf{0.2}\}$ (day^{-1})	Fixed
m	Cyst mortality rate	$\mathbf{10}^{-5}$ (day^{-1})	Fixed
ζ	Cyst burial rate	$\{10^{-3}, \mathbf{10}^{-2}, 10^{-1}\}$ (day^{-1})	Fixed
γ	Germination \times Resuspension rate	$\{10^{-3}, \mathbf{10}^{-2}, 10^{-1}\} \times \{10^{-5}, 10^{-3}, \mathbf{10}^{-1}\}$ (day^{-1})	Fixed

Table 1: Definition of main state variables and model parameters. State variables and fluctuating parameters are indicated in the last column as “Dynamic”. Parameters that are constant through time are either “Fixed” (directly obtained from literature) or “Calibrated” (obtained through model fitting, with initial values arising from previous studies at the study site). When a range of values is given, the bold numbers indicate the reference values while the others are used for sensitivity analysis. $\beta(0.55, 1.25)$ is the Beta distribution with parameters 0.55 and 1.25. For γ , germination values for sensitivity analysis were multiplied by the reference value for resuspension, and conversely.

Each compartment (ocean, coast, cyst bank) contains 10^3 cells at the beginning of the simula-

tion, and the dynamics are run for 30 years with a daily time step. We model the temperature input as a noisy sinusoidal signal with the same mean and variance as the empirical data set described below: the amplitude of the sinusoid is 12.4°C and the standard deviation of the noise is 0.25°C .

Parameterization of the models

Literature-derived parameter values

Loss rate The loss rate of vegetative cells can be attributed to natural mortality, predation or parasitism. This rate is quite variable in the literature: the model of Scranton & Vasseur (2016) considered a rate around 0.04 day^{-1} while a review by Sarthou *et al.* (2005) indicates a grazing rate of the standing stock between 0.2 and 1.8 day^{-1} and an autolysis rate between 0.005 and 0.24 day^{-1} (in the absence of nutrients, or because of viral charge). A maximum value of 0.2 is fixed for the model (see Section S3 of the SI for more details).

Sinking rate Phytoplanktonic particles have a higher density than water and cannot swim to prevent sinking (although they are able to regulate their buoyancy, Reynolds 2006). Sinking is mostly affected by hydrodynamics, but at the species-level, size, shape, density-regulation and colony-formation capabilities are key determinants of the particle flotation. In this model, the sinking rate of each species cysts is drawn from a Beta distribution with a mean value of 9% , and a maximum (S_{\max}) around 30% , that is $s \sim 0.3\beta(0.55, 1.25)$ (see Fig. S4), adapted from observations by Passow (1991) and Wiedmann *et al.* (2016).

Exchange rate The exchange rate between the ocean and the coast depends on the shape and location of the coast (estuary, cape, ...). Our calibration site is located at an inlet. The flow at the inlet leads to a renewal time of the coastal area water evaluated between 1 and 2.5 days (Ascione Kenov *et al.*, 2015), which corresponds to a daily exchange rate between 40 and 100% .

Cyst mortality and burial Cyst loss is the result of cyst mortality m and burial by sedimentation ζ . Mortality values range between 10^{-5} and 10^{-4} per day (more details on the approximation of mortality rates from McQuoid *et al.* 2002 are given in Section S3 of the SI). However, cyst burial by sedimentation is the prevailing phenomenon. Indeed, once cysts have been buried, they are not accessible for resuspension even if they could still germinate. Burial depends on the hydrodynamics of the site, but also on biotic processes (i.e., bioturbation) and anthropogenic disturbances such as fishing or leisure activities (e.g., jet skiing). This parameter is thus heavily dependent on the environmental context and varies here between 0.001 and 0.1 per day.

Germination/resuspension Both resuspension and germination are needed for cysts to contribute to the vegetative pool in the water column ($\gamma = \text{resuspension} \times \text{germination}$). Following McQuoid *et al.* (2002) and Agrawal (2009), we assume a temperature threshold: germination is triggered by temperatures going above 15°C. As actual rates of germination are not easily deduced from the literature, a set of credible values has been tested (1%, 0.1%, 0.01%). Similarly, resuspension values are seldom computed for phytoplanktonic cells, but models for inorganic particles can be used (see Section S3 of the SI for literature and details). In this paper, we explore values between 10^{-5} (stratified water column) to 0.1 (highly mixed environment).

Parameter calibration

We use initial interaction estimates from our previous time series modelling study (Picoche & Barraquand, 2020, see Section S3 of the SI for the equations). These initial interaction estimates are then calibrated to the time series (see below), to take into account the differences in model structure and timescale between this study and Picoche & Barraquand (2020).

The calibration procedure consists in launching 1000 simulations, each characterized by a specific set of interaction coefficients. More precisely, for each simulation, an interaction

coefficient (α_{ij} in model I, H_{ij} in model II) has probability $\frac{1}{5}$ to keep its present value, probability $\frac{1}{5}$ to increase by 10%, $\frac{1}{5}$ to decrease by 10%, $\frac{1}{5}$ to be halved and $\frac{1}{5}$ to be doubled. The numbers of coastal pelagic cells (which are the ones measured empirically) are then extracted over the last 2 years of the simulation, and compared to observations using the following summary statistics:

- average abundance $f_1 = \sqrt{\frac{1}{S} \sum_i^S (\bar{n}_{i,obs} - \bar{n}_{i,sim})^2}$ where S is the number of taxa and \bar{n}_i is the logarithm of the mean abundance of taxon i
- amplitude of the cycles $f_2 = \sqrt{\frac{1}{S} \sum_i^S [(\max(n_{i,obs}) - \min(n_{i,obs})) - (\max(n_{i,sim}) - \min(n_{i,sim}))]^2}$ where n_i is the logarithm of the abundance of taxon i .
- period of the bloom. The year is divided in 3 periods, i.e. summer, winter and the spring/autumn group (as taxa blooming in these periods can appear in either or both seasons). We give a score of 0 if the taxon blooms in the same period as its observed counterpart and 1 otherwise.

Simulations with taxon extinction (i.e., the taxon is absent for more than 6 months in a compartment) are discarded, as extinctions are not observed in the field data. Parameter sets are then ranked according to their performance for each summary statistic, and we select the set of interactions minimizing the sum of the ranks.

Sensitivity analysis Parameters taken from the literature may be site- or model- specific, or vary over one order of magnitude in the literature, e.g., rates of sinking s , resuspension/germination γ , cyst burial ζ , and loss of pelagic cells l . We therefore performed a sensitivity analysis to these highly uncertain parameters. The set of tested values for each parameter is given in Table 1. We used average abundances and amplitudes at the community and taxon levels for the last 2 years of simulations as the major model diagnostics.

Empirical dataset used for calibration

The models are calibrated using time series of phytoplanktonic abundances that have been monitored biweekly for 21 years in the Marennes-Oléron Bay, on the French Atlantic Coast (the Auger site analysed in Picoche & Barraquand, 2020). This dataset – like most other plankton monitoring studies – has a slightly coarser taxonomy than our mechanistic model. We stress that we are not trying to model precisely this particular community, but rather to constrain our models to produce lifelike patterns of phytoplankton community dynamics.

Scenarii

The effect of the cyst bank on biodiversity and community dynamics can be evaluated through the response to disturbance with and without the cyst compartment. Cyst mortality is set to 100% to remove the cyst bank. We evaluate two main disturbances:

1. increase or decrease in interaction strength
2. temperature change, either in mean value or variability

In the first scenario, interaction strengths are multiplied or divided by a factor ranging between 1 and 10. In order to differentiate the effects of facilitative and competitive interactions on coexistence, we only vary only one type of interactions at a time. Here, both intra and interspecies interactions are modified; we present in Section S6 of the SI additional simulations with a change in interspecies interactions only.

In the second scenario, five different climate change trajectories are assessed. In the first three, the average temperature is increased by 2, 5, or 7°C (Boucher *et al.*, 2020). In the next two, keeping the reference average temperature, the total variance of the temperature, including seasonality and noise, is either decreased or increased by 25%. Each climate change trajectory is run 5 times to account for the intrinsic stochasticity of the temperature signal.

In both scenarios, simulations are run for 30 years for both population growth models, with and without a cyst compartment, and only the last 2 years are considered to evaluate effects of changes in parameters and in temperature. The code for all simulations is to be found at <https://github.com/CoraliePicoche/SeedBank>.

Results

Phytoplankton dynamics

The classical mass-action (model I) and saturating interaction (model II) formulations of multispecies dynamics both reproduced the main characteristics of observed phytoplankton dynamics. They produced one or two blooms during the year and a range of abundances covering several orders of magnitude, with the right timing of the blooms. At the Auger site that was used for calibration, abundances increase in spring and can last over part of summer, or start a new bloom in autumn, which is what we observed as well in the models. Annual mean abundance of the various taxa was also well reproduced. That said, in some cases, abundances could be lower than expected and the variation in abundances due to seasonality was underestimated (Fig. 2). In all cases, saturating interactions led to higher abundances than mass-action interactions throughout the year (Fig. S5).

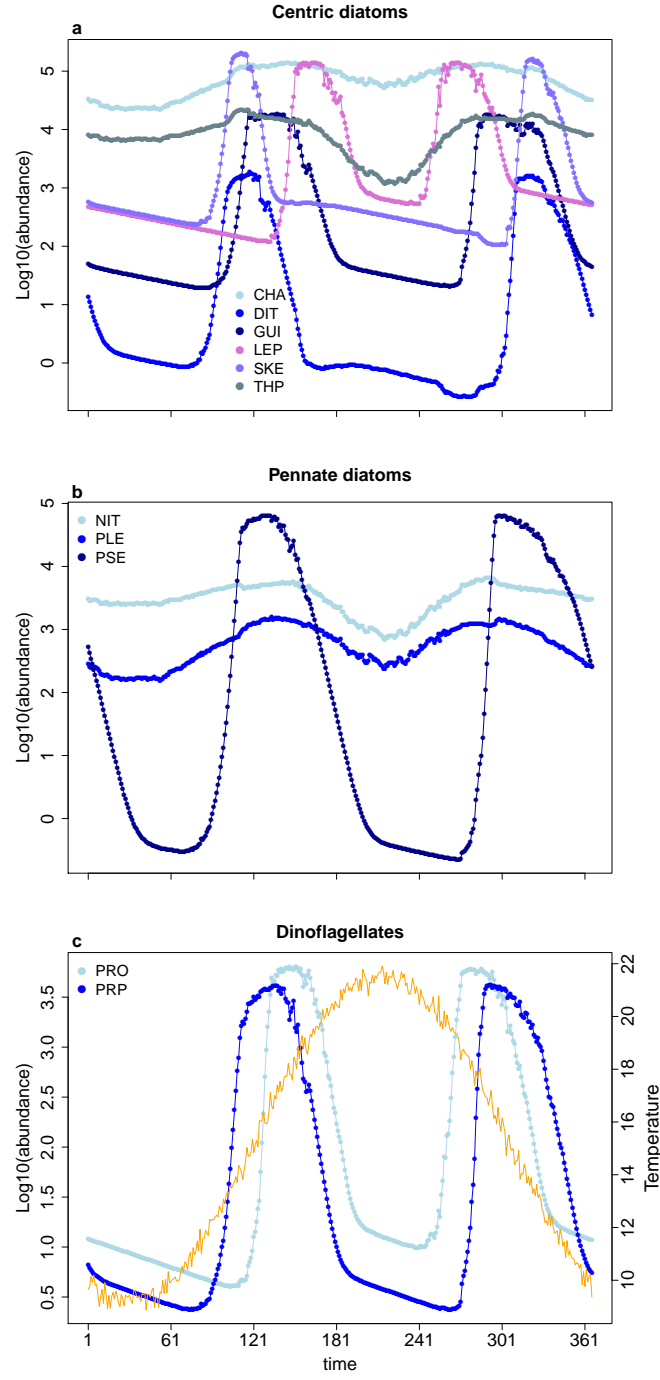


Figure 2: Simulated phytoplankton dynamics for a year in model I. Each panel corresponds to a cluster of interacting taxa. The orange line in the third panel indicates the temperature.

Sensitivity to uncalibrated parameters

Phytoplankton dynamics were not strongly affected by changes in the parameter values (Fig. 3). As parameters were varied in their plausible range, the average change in mean abundance on the coast between the reference simulation and the sensitivity simulations varied between -4.6 and 1.9% for model I and between -4.2 and 1.1% for model II, with similar deviations (same sign and magnitude) in the two models. In the two models, the decrease in mortality rate of vegetative cells l had the highest impact on the final average abundance, leading to an increase in abundances. The exchange rate between the ocean and the coast had much less effect on the coastal average abundance.

On the other hand, the amplitude (i.e., decimal logarithm of the maximum to minimum ratio of abundance) was more affected by changes in parameters and could vary by -39.4 to 18.6% in model I, and between -41.2% and 23% in model II. Results were qualitatively the same in the two models, with a decrease in cyst burial being the main driver of the decrease in amplitude, and a decrease in resuspension leading to an increase in amplitude.

In three cases (cyst burial rate set to 0.1, resuspension to 10^{-5} or exchange rate set to 0), the final richness of the oceanic community decreased from 11 to 4. Extant species were the same in all simulations (CHA, THP, NIT, PSE). When resuspension was set to 0.001, a species periodically disappeared from the ocean, to be subsequently re-seeded by the coastal population.

For all parameters, except the sinking rate, an increase in mean abundance was associated to a decrease in amplitude.

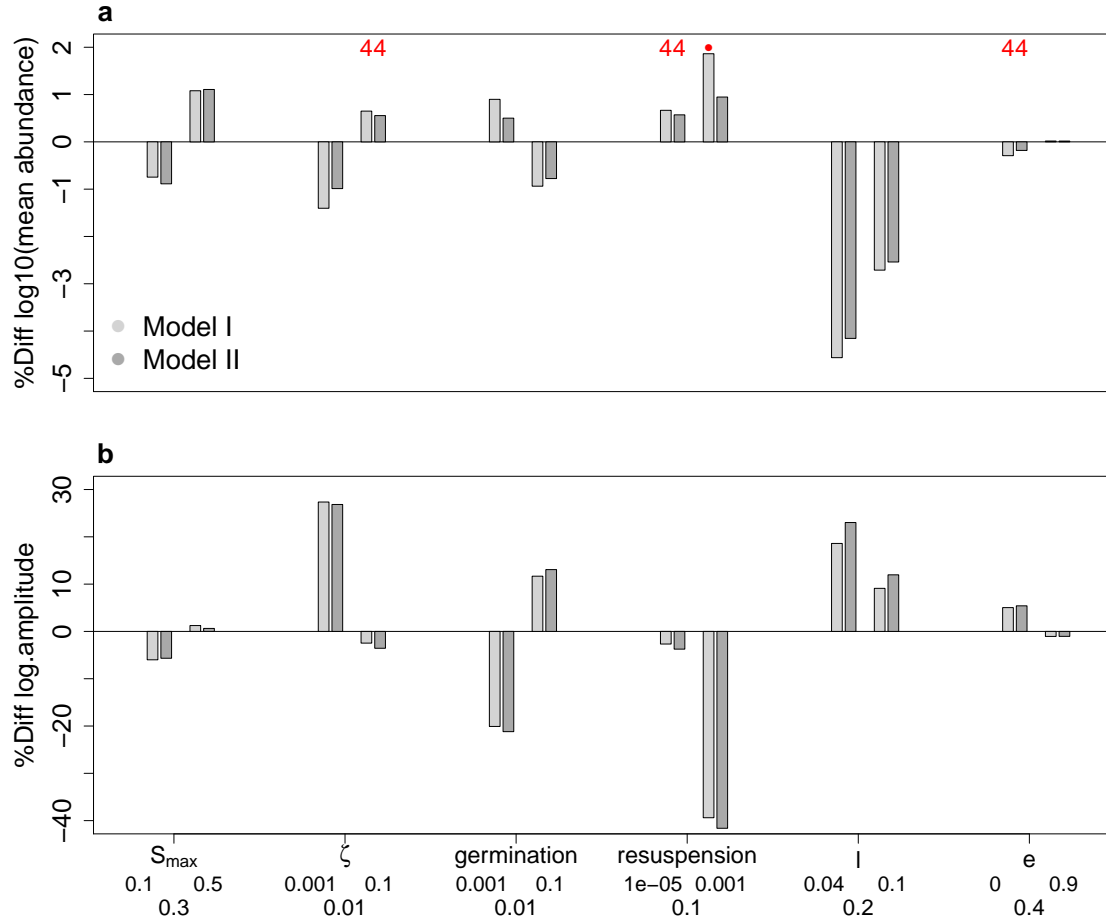


Figure 3: Sensitivity of the model to variation in parameters, measured as the difference between the reference simulation metric and the metric for the simulation including a change in parameter. The two metrics used were the average decimal log abundance (a) and the decimal logarithm of the ratio between maximum and minimum abundance (b) of the coastal phytoplanktonic community. Values used in the sensitivity analysis are in the second row of the x-axis while values used in the reference simulation are shown in the third row. Note that the reference value is not necessarily within the range of values used in the sensitivity analysis (e.g. mortality rates in the sensitivity analysis are both below the value used in other simulations). Numbers in red are the final number of species in the ocean and dots correspond to simulations in which at least one species reached 0 at one point but did not disappear.

Scenarios of environmental change

Two scenarios were designed to test the buffering effect of the cyst bank against disruption. In both cases, it consisted in removing the cyst bank by setting cyst mortality to 100% per

day. Without any other disturbance to the system, this led to a decrease in richness from 11 to 4 species at the end of the simulation (Fig. 4) while the total abundance of phytoplankton was not strongly affected (around 10^5 in all cases). The inverse of the Simpson index (the second Hill number) decreased from approximately 3 to 1, showing that the disappearance of the cyst bank did not affect only the rarest species.

Biotic effects

Our first hypothesis was that the absence of the cyst bank would cause the community to be more affected by a higher competition strength. Counter-intuitively, our results (Fig. 4) showed that an increase in competition strength only had negative effects with model I, and for high competition values (6 times the reference ones at least), shifting from 4 to 3 species in the oceanic compartment of a community without cyst bank. By contrast, an increase in competition strength did not affect the richness of a community with a cyst bank. On the contrary, a decrease in competition (from a factor 0.5 and lower) or an increase in facilitation (starting from a factor 2 and higher) led to much smaller communities in model II in the absence of a cyst bank, sometimes with a complete competitive exclusion. Richness was lowest when competition was divided by 6 or when facilitation was multiplied by 8 in model II. The same pattern (richness stability with model I, sensitivity to a decrease in competition or an increase in facilitation with model II) was observed in a community with a cyst bank, but for larger disturbances. Competition indeed had to be at least divided by 6 or facilitation, to be multiplied by 7 for richness to decrease to 9 species.

The inverse of the Simpson index was also affected by the changes in interaction strengths, with similar patterns to richness, as it was lowest for high facilitation or low competition. Presumably some species reach very high growth rates in these scenarios, which then feeds back onto community dynamics, generating lower diversity in the end.

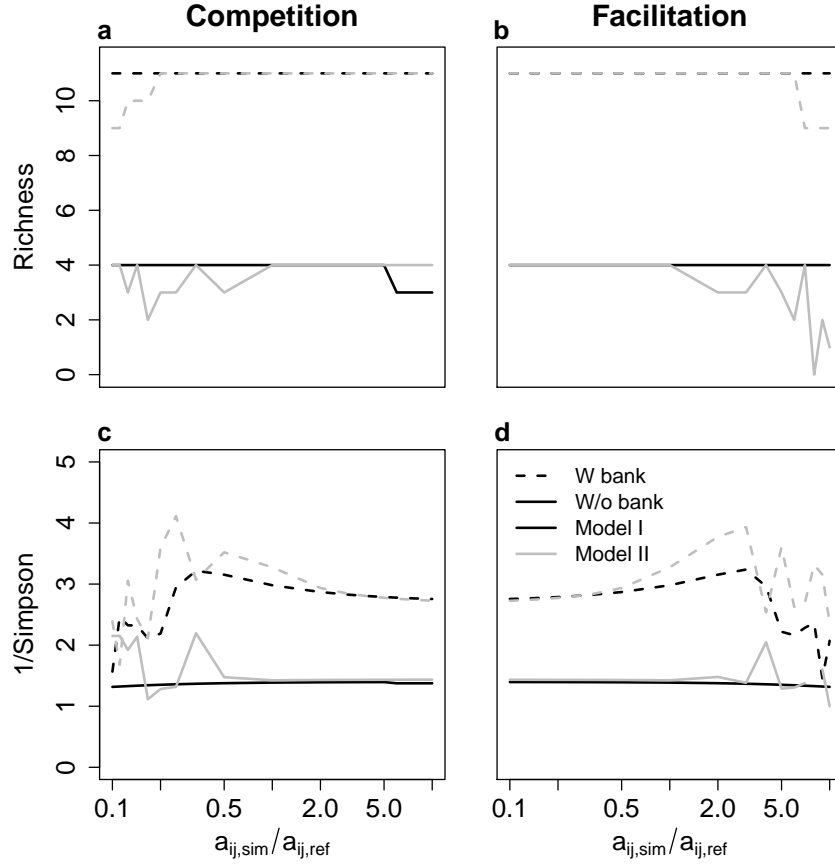


Figure 4: Measures of biodiversity in the ocean at the end of the simulation: a-b) richness and c-d) inverse of the Simpson index, with (dashed line) and without (solid line) a cyst bank, as a function of the strength of competition and facilitation with a classical Beverton-Holt (black lines) or a saturating interaction (grey lines) formulation. The x-axis shows the factor by which each interaction was multiplied (note the logarithmic scale).

Taxa which disappear were always the same and were characterized by a lower minimum abundance, a higher amplitude of fluctuations and a small niche (Fig. 5). In contrast, their interactions were not qualitatively different from the other species.

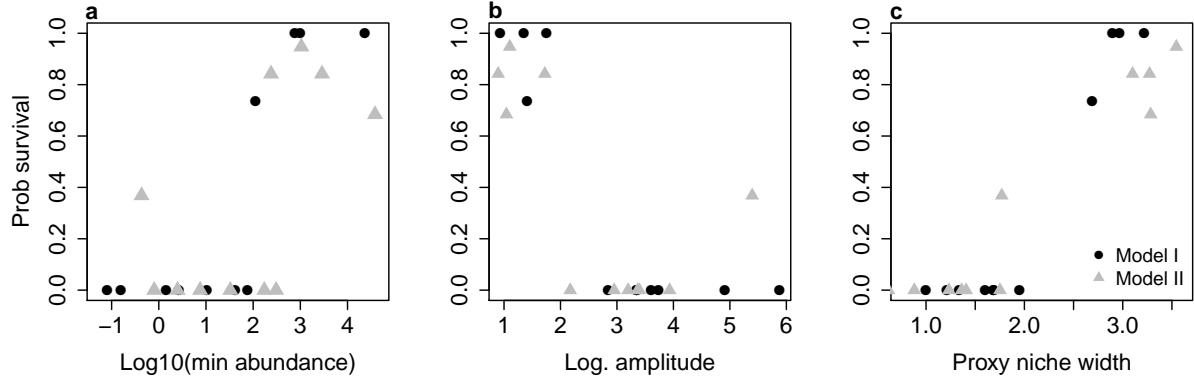


Figure 5: Probability of survival of species when competition increases in the absence of a cyst bank, as a function of their dynamics characteristics (minimum abundance, logarithm of amplitude and niche width) in the reference parameter set.

Abiotic effects

Our second hypothesis was that the absence of a cyst bank would reduce the ability of a community to withstand changes in its abiotic environment, here represented by variation in the temperature. This was true for both models (Fig. 6), as the communities without a cyst bank could not maintain their richness with an increase in temperature above 2°C , as opposed to communities with a cyst bank, which could only be affected by a 7°C increase (scenario SSP5 8.5, Boucher *et al.* 2020). In all cases however, the total abundances were not strongly affected. Indeed, the total abundance of a community is driven by a small number of numerically dominant species, which did not disappear. High total abundances tended to correspond to the abundance of only one or two species. Model II consistently led to higher abundances, as was already the case in the reference simulations.

The variance of the temperature did not affect richness nor total abundance of communities with a cyst bank. This was also true without a cyst bank. The presence of the cyst bank did increase total abundance though.

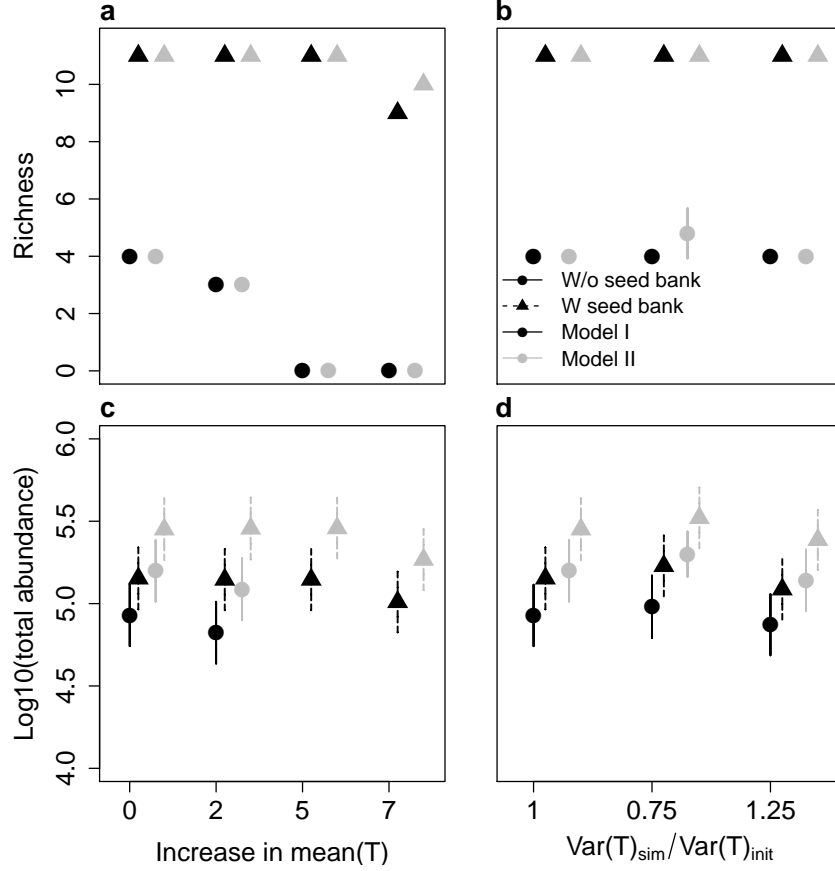


Figure 6: Variation in richness and total abundance with and without a cyst bank as a function of the mean (left) and variance (right) of the temperature with a mass-action (black line, model I) or a saturating interaction (grey line, model II) formulation.

Discussion

Using a meta-community model which accounts for exchanges between the ocean and the coast, as well as movements between the top and the bottom of the coastal water column, we were able to show that a specific life stage, the seed – or cyst – stage, can help maintain biodiversity. This dormant stage was integrated to a phytoplanktonic community dynamics model, which was parameterized based on literature, field-based phenology, and interaction strength estimates. The model was then calibrated on phytoplankton community time series. Our model was able to simulate realistic community dynamics (both mean abundances and temporal patterns), while including the effects of both positive and negative interactions

on community dynamics. When removing the cyst bank, biodiversity decreased drastically. This was true for the reference parameter values, as well as when species interaction strengths and environmental fluctuation levels were altered, in which cases the cyst bank’s buffering influence disappeared. The total abundance of the community decreased as well. Moreover, when faced with a biotic or abiotic “press” perturbation, communities where species could divert part of their population to a dormant stage were less prone to species loss and could maintain their biomass through the years. These results were consistent for the two interaction models that we considered, with and without progressive saturation in interaction strengths. Our results therefore demonstrate the major potential role of phytoplanktonic cyst banks in maintaining biodiversity. These results align with the findings of previous theoretical studies, that have put forward similar effects of dormant stages in other taxa, such as plants (Levine & Rees, 2004; Jabot & Pottier, 2017), invertebrates (Wisnoski *et al.*, 2019) or (smaller) microbes (Jones & Lennon, 2010).

The effect of the cyst bank is, of course, contingent upon a long dormancy of the cyst stage. Dormancy has long been observed in field and experimental data, including for phytoplanktonic organisms (Eilertsen & Wyatt, 2000). It has been theorized to be an important and neglected process in the wider microbiology literature (Locey, 2010; Jones & Lennon, 2010). Processes behind diversity maintenance by the seed stage include the storage effect (Facelli *et al.*, 2005; Angert *et al.*, 2009; Bonis *et al.*, 1995) but are not limited to it. This is because a long dormancy alone can allow future recolonization of a community where counts of pelagic cells alone would suggest that some species have gone extinct. This colonization-in-time may of course combine with present recolonization from other spatial areas (Shmida & Ellner, 1984). In our case, our focus on phytoplankton led us to assume that organisms moved between the coast and the ocean, which were largely synchronous environments. Spatial recolonization was therefore less important than temporal recolonization; the relative importance of the two processes may vary depending on the organisms and the degree of spatial synchrony of their environment.

The specificities of phytoplankton cysts, that usually fall to the ocean bottom in coastal areas, led us to assume that only the “vegetative” stage (here, the classic pelagic form of planktonic cells) disperse. In some other metacommunity models with dormant seed banks (e.g. Wisnoski *et al.*, 2019), the dormant stage can disperse as well. This would be true for most plants too (and perhaps some phytoplankters in situations where they are transported by animals). However, the restriction about which stage can move did not change the general conclusion of Wisnoski *et al.* (2019): the combination of spatial dispersal and dormancy through seed banks greatly helps biodiversity maintenance. In our study, this main result was also robust to changes in exchange parameters and mean interaction values in the community.

The various species present in the community had different survival probabilities in the absence of a seed bank. Some species could persist without a cyst bank while others could not (which confirms conclusions from Hellweger *et al.* 2008 for single species). Other species periodically disappeared from the community in the open ocean, while being able to reinvade the coast which connected to the cyst bank. This suggests that some species may be locally transient: they are filtered out from certain patches, but can reinvade more or less periodically the environment (Guittar *et al.*, 2020). Certain species characteristics could explain species extinction, whether definitive or only temporary: higher amplitudes of population variation were typically associated with extinctions. We identified, by studying realised population growth rates (Fig. S7 in SI), that a smaller niche width (i.e., being a specialist) or being strongly affected by species interactions can explain rapid extinction without a cyst bank.

Despite the evidence for seed bank effects that we and others uncovered, phytoplanktonic community models designed to explain biodiversity usually avoid modelling seed/cyst banks. In our view, this may decrease the possibility of spontaneous re-colonization at the coast (at very low densities initially), which can then spill to the open ocean by progressive dispersal by the currents. If the goal of a community-level model is very short-term prediction (days, weeks), this recolonization can probably be neglected. However, over multiple years, ignoring cryptic stages allowing recolonization could strongly bias our view of long-term coexistence.

Long-term phytoplankton coexistence modelling (over multiple decades or more) likely requires that we take into account cysts, whose influence may become only more important as the timescale increases, due to the very long possible dormancies that have been evidenced (Ellegaard & Ribeiro, 2018; Sanyal *et al.*, 2018). When modelling different stages of the life cycle in a detailed manner – as done here – is impractical, the recolonization could perhaps be simplified to a stochastic immigration term (as done in Stock *et al.* 2005 in a single-species context). This technical suggestion certainly extends to models of (terrestrial) plant community dynamics.

More research on dormant stages may be needed to parameterize truly predictive mechanistic phytoplankton models with multiple life stages, in particular to inform parameters such as the sinking rate of resting cells, as well as burial and resuspension parameters. These parameters are all linked to hydrodynamics (Yamamoto *et al.*, 2002; Yñíguez *et al.*, 2012) and may locally vary. Sinking rates show an interesting conflict between short- and long-term survival: in coastal areas, a fraction of sinking cells contribute to the cyst bank, increasing the odds of species long-term survival at the cost of short-term individual cell survival. But high sinking rates are essentially “wasted” in the open ocean – whether different sinking rates can be selected, to some degree, by such different environments could be quite revealing. How cells get up rather than down in water column might be as interesting but more difficult to study. The likely idiosyncratic nature of recolonization by cysts – due to the contingency on local hydrodynamics – means that experimentation might be the only manner in which the frequency of reinvasion can be assessed. Currently, one of the only parameters measured in the field is the rate of survival of the cells found in the sediment (Montresor *et al.*, 2013; Solow *et al.*, 2014). While very important, this parameter is a necessary not sufficient condition for reinvasion of the population at future times. We need more information about the abilities of cysts buried in the sediment to come up to the pelagic zone, which is required for recolonization to actually occur. Many factors may contribute: bottom currents, benthic animals, ... We therefore encourage both experiments and field observations to follow actual

seed trajectories, in order to help us understand this cryptic part of the diversity maintenance process.

Acknowledgements

We thank Nathan Wisnoski and Frank Jabot for useful feedback. FB and CP were supported by the French ANR through LabEx COTE (ANR-10-LABX-45). CP was supported by a PhD grant from the French Ministry of Research.

References

- Agrawal, S.C. (2009). Factors affecting spore germination in algae - review. *Folia Microbiologica*, 54, 273–302.
- Aikio, S., Ranta, E., Kaitala, V. & Lundberg, P. (2002). Seed bank in annuals: Competition between banker and non-banker morphs. *Journal of Theoretical Biology*, 217, 341–349.
- Angert, A.L., Huxman, T.E., Chesson, P. & Venable, D.L. (2009). Functional tradeoffs determine species coexistence via the storage effect. *PNAS*, 106, 11641–11645.
- Ascione Kenov, I., Muttin, F., Campbell, R., Fernandes, R., Campuzano, F., Machado, F., Franz, G. & Neves, R. (2015). Water fluxes and renewal rates at Pertuis d’Antioche/Marennes-Oléron Bay, France. *Estuarine, Coastal and Shelf Science*, 167, 32–44.
- Azanza, R.V., Brosnahan, M.L., Anderson, D.M., Hense, I. & Montresor, M. (2018). The role of life cycle characteristics in harmful algal bloom dynamics. In: *Global Ecology and Oceanography of Harmful Algal Blooms* (eds. Glibert, P.M., Berdalet, E., Burford, M.A., Pitcher, G.C. & Zhou, M.). Springer International Publishing, Cham, vol. 232, pp. 133–161.
- Batifoulier, F., Lazure, P., Velo-Suarez, L., Maurer, D., Bonneton, P., Charria, G., Dupuy, C.

- & Gentien, P. (2013). Distribution of *Dinophysis* species in the Bay of Biscay and possible transport pathways to Arcachon Bay. *Journal of Marine Systems*, 109-110, S273–S283.
- Bissinger, J., Montagnes, D., Harples, J. & Atkinson, D. (2008). Predicting marine phytoplankton maximum growth rates from temperature: Improving on the Eppley curve using quantile regression. *Limnology and Oceanography*, 53, 487–493.
- Bonis, A., Lepart, J. & Grillas, P. (1995). Seed bank dynamics and coexistence of annual macrophytes in a temporary and variable habitat. *Oikos*, 74, 81.
- Boucher, O. *et al.* (2020). Presentation and evaluation of the IPSL-CM6A-LR Climate Model. *Journal of Advances in Modeling Earth Systems*, 12.
- Cáceres, C.E. (1997). Temporal variation, dormancy, and coexistence: A field test of the storage effect. *Proceedings of the National Academy of Sciences*, 94, 9171–9175.
- Chesson, P. (2000). Mechanisms of maintenance of species diversity. *Annual review of Ecology and Systematics*, pp. 343–366.
- Chesson, P. (2018). Updates on mechanisms of maintenance of species diversity. *Journal of Ecology*, 106, 1773–1794.
- Chesson, P. & Huntly, N. (1988). Community consequences of life-history traits in a variable environment. *Annales Zoologici Fennici*, 25, 5–16.
- Chu, C. & Adler, P.B. (2015). Large niche differences emerge at the recruitment stage to stabilize grassland coexistence. *Ecological Monographs*, 85, 373–392.
- Comita, L.S., Muller-Landau, H.C., Aguilar, S. & Hubbell, S.P. (2010). Asymmetric density dependence shapes species abundances in a tropical tree community. *Science*, 329, 330–332.
- Cushing, J.M., Leverage, S., Chitnis, N. & Henson, S.M. (2004). Some discrete competition models and the competitive exclusion principle. *Journal of difference Equations and Applications*, 10, 1139–1151.

- Eilertsen, H. & Wyatt, T. (2000). Phytoplankton models and life history strategies. *South African Journal of Marine Science*, 22, 323–337.
- Ellegaard, M. & Ribeiro, S. (2018). The long-term persistence of phytoplankton resting stages in aquatic ‘seed banks’. *Biological Reviews*, 93, 166–183.
- Ellner, S. (1987). Alternate plant life history strategies and coexistence in randomly varying environments. *Vegetatio*, 69, 199–208.
- Estrada, M., Solé, J., Anglès, S. & Garcés, E. (2010). The role of resting cysts in *Alexandrium minutum* population dynamics. *Deep Sea Research Part II: Topical Studies in Oceanography*, 57, 308–321.
- Facelli, J.M., Chesson, P. & Barnes, N. (2005). Differences in seed biology of annual plants in arid lands: A key ingredient of the storage effect. *Ecology*, 86, 2998–3006.
- Fujiwara, M., Pfeiffer, G., Boggess, M., Day, S. & Walton, J. (2011). Coexistence of competing stage-structured populations. *Scientific Reports*, 1.
- Guittar, J., Goldberg, D., Klanderud, K., Berge, A., Boixaderas, M.R., Meineri, E., Töpper, J. & Vandvik, V. (2020). Quantifying the roles of seed dispersal, filtering, and climate on regional patterns of grassland biodiversity. *Ecology*, 101, e03061.
- Hellweger, F.L., Kravchuk, E.S., Novotny, V. & Gladyshev, M.I. (2008). Agent-based modeling of the complex life cycle of a cyanobacterium (*Anabaena*) in a shallow reservoir. *Limnology and Oceanography*, 53, 1227–1241.
- Hense, I. & Beckmann, A. (2006). Towards a model of cyanobacteria life cycle-effects of growing and resting stages on bloom formation of N₂-fixing species. *Ecological Modelling*, 195, 205–218.
- Huang, Z., Liu, S., Bradford, K.J., Huxman, T.E. & Venable, D.L. (2016). The contribution of

- germination functional traits to population dynamics of a desert plant community. *Ecology*, 97, 250–261.
- Jabot, F. & Pottier, J. (2017). Macroecology of seed banks: The role of biogeography, environmental stochasticity and sampling. *Global Ecology and Biogeography*, 26, 1247–1257.
- Jones, S.E. & Lennon, J.T. (2010). Dormancy contributes to the maintenance of microbial diversity. *PNAS*, 107, 5881–5886.
- Lee, S., Hofmeister, R. & Hense, I. (2018). The role of life cycle processes on phytoplankton spring bloom composition: a modelling study applied to the Gulf of Finland. *Journal of Marine Systems*, 178, 75–85.
- Levine, J.M. & Rees, M. (2004). Effects of temporal variability on rare plant persistence in annual systems. *The American Naturalist*, 164, 350–363.
- Locey, K.J. (2010). Synthesizing traditional biogeography with microbial ecology: the importance of dormancy. *Journal of Biogeography*, 37, 1835–1841.
- Marcus, N. & Boero, F. (1998). Minireview: The importance of benthic-pelagic coupling and the forgotten role of life cycles in coastal aquatic systems. *Limnology and Oceanography*, 43, 763–768.
- Margalef, R. (1978). Life-forms of phytoplankton as survival alternatives in an unstable environment. *Oceanologica acta*, 1, 493–509.
- Martorell, C. & Freckleton, R.P. (2014). Testing the roles of competition, facilitation and stochasticity on community structure in a species-rich assemblage. *Journal of Ecology*, 102, 74–85.
- May, R.M. (1981). *Theoretical Ecology: Principles and Applications*. Oxford University Press UK.

- McGillicuddy, D., Anderson, D., Lynch, D. & Townsend, D. (2005). Mechanisms regulating large-scale seasonal fluctuations in *Alexandrium fundyense* populations in the Gulf of Maine: Results from a physical-biological model. *Deep Sea Research Part II: Topical Studies in Oceanography*, 52, 2698–2714.
- McQuoid, M.R., Godhe, A. & Nordberg, K. (2002). Viability of phytoplankton resting stages in the sediments of a coastal Swedish fjord. *European Journal Phycology*, 37, 191–201.
- Moll, J. & Brown, J. (2008). Competition and coexistence with multiple life-history stages. *The American Naturalist*, 171, 839–843.
- Montresor, M., Di Prisco, C., Sarno, D., Margiotta, F. & Zingone, A. (2013). Diversity and germination patterns of diatom resting stages at a coastal Mediterranean site. *Marine Ecology Progress Series*, 484, 79–95.
- Passow, U. (1991). Species-specific sedimentation and sinking velocities of diatoms. *Marine Biology*, 108, 449–455.
- Patrick, R. (1948). Factors effecting the distribution of diatoms. *Botanical Review*, 14, 473–524.
- Picoche, C. & Barraquand, F. (2020). Strong self-regulation and widespread facilitative interactions between genera of phytoplankton. *Journal of Ecology*.
- Qian, J. & Akçay, E. (2020). The balance of interaction types determines the assembly and stability of ecological communities. *Nature Ecology & Evolution*, 4, 356–365.
- Reynolds, C.S. (2006). *The ecology of phytoplankton*. Cambridge University Press.
- Sanyal, A., Larsson, J., van Wirdum, F., Andrén, T., Moros, M., Lönn, M. & Andrén, E. (2018). Not dead yet: Diatom resting spores can survive in nature for several millennia. preprint, bioRxiv.

- Sarthou, G., Timmermans, K.R., Blain, S. & Tréguer, P. (2005). Growth physiology and fate of diatoms in the ocean: a review. *Journal of Sea Research*, 53, 25–42.
- Scranton, K. & Vasseur, D.A. (2016). Coexistence and emergent neutrality generate synchrony among competitors in fluctuating environments. *Theoretical Ecology*, 9, 353–363.
- Shmida, A. & Ellner, S. (1984). Coexistence of plant species with similar niches. *Vegetatio*, 58, 29–55.
- Shoemaker, L.G. & Melbourne, B.A. (2016). Linking metacommunity paradigms to spatial coexistence mechanisms. *Ecology*, 97, 2436–2446.
- Smayda, T.J. & Reynolds, C.S. (2001). Community assembly in marine phytoplankton: application of recent models to harmful dinoflagellate blooms. *Journal of Plankton Research*, 23, 447–461.
- Solow, A., Beet, A., Keafer, B. & Anderson, D. (2014). Testing for simple structure in a spatial time series with an application to the distribution of *Alexandrium* resting cysts in the Gulf of Maine. *Marine Ecology Progress Series*, 501, 291–296.
- Stock, C.A., McGillicuddy, D.J., Solow, A.R. & Anderson, D.M. (2005). Evaluating hypotheses for the initiation and development of *Alexandrium fundyense* blooms in the western Gulf of Maine using a coupled physical-biological model. *Deep Sea Research Part II: Topical Studies in Oceanography*, 52, 2715–2744.
- Tester, P.A. & Steidinger, K.A. (1997). *Gymnodinium breve* red tide blooms: Initiation, transport, and consequences of surface circulation. *Limnology Oceanography*, 42, 1039–1051.
- Wiedmann, I., Reigstad, M., Marquardt, M., Vader, A. & Gabrielsen, T. (2016). Seasonality of vertical flux and sinking particle characteristics in an ice-free high arctic fjord-Different from subarctic fjords? *Journal of Marine Systems*, 154, 192–205.

- Wisnoski, N.I., Leibold, M.A. & Lennon, J.T. (2019). Dormancy in metacommunities. *The American Naturalist*, 194, 135–151.
- Yñiguez, A., Cayetano, A., Villanoy, C., Alabia, I., Fernandez, I., Palermo, J., Benico, G., Siringan, F. & Azanza, R. (2012). Investigating the roles of intrinsic and extrinsic factors in the blooms of *Pyrodinium bahamense* var. *compressum* using an individual-based model. *Procedia Environmental Sciences*, 13, 1462–1476.
- Yamamoto, T., Seike, T., Hashimoto, T. & Tarutani, K. (2002). Modelling the population dynamics of the toxic dinoflagellate *Alexandrium tamarense* in Hiroshima Bay, Japan. *Journal of Plankton Research*, 24, 33–47.

Supporting Information for *Seed banks can help to maintain the diversity of interacting phytoplankton species* by C. Picoche & F. Barraquand.

S1 Intrinsic growth rate modeling

The intrinsic growth rate can be decomposed in 2 elements:

$$r_i(T) = E(T)f_i(T) \quad (1)$$

with $E(T)$ the response to temperature common to all species and $f_i(T)$ the species-specific response. This section provides detailed information regarding $E(T)$ and $f_i(T)$ estimates that affect the realized growth rate of phytoplanktonic organisms in a community.

Common response to temperature

Phytoplanktonic growth rates cover a broad range of values: between 0.2 and 1.78 day⁻¹ for diatoms in Reynolds (2006), even reaching 3 day⁻¹ in the meta-analysis of 308 experiments by Edwards *et al.* (2015). These values are often computed from measurements on isolated species or on small communities in laboratory conditions, in a constant environment. A broader perspective is therefore necessary to understand general responses to changes in the environment (Bissinger *et al.*, 2008; Edwards *et al.*, 2016), especially temperature.

We first used the equation by Scranton & Vasseur (2016) as a starting point, but it was not able to reproduce the observed values found in Edwards *et al.* (2015) (see low values of the growth rate in Fig. S1a, between 0.05 and 0.8, in place of values between 0.2 and 3 day⁻¹). In this context, we decided to use the formula by Bissinger *et al.* (2008) to compute the maximum growth rate response to the temperature. There are two reasons for this choice. First, their model is a general function that can be applied to all species. Second, Bissinger *et al.* (2008) is an update of the seminal work of Eppley (1972) which was used in Scranton & Vasseur (2016), but might be outdated.

The relationship between temperature and growth rate is then $E(T) = 0.81e^{0.0631(T-273.15)}$, with T in Kelvin degrees. In this case, growth rates vary between 0.81 and 3.9 day⁻¹ for temperatures between 0 and 25°C, in line with previous observations. However, these daily growth rates need to be proportional to the daylength as no growth occurs at night: we therefore divide $E(T)$ by two in our models.

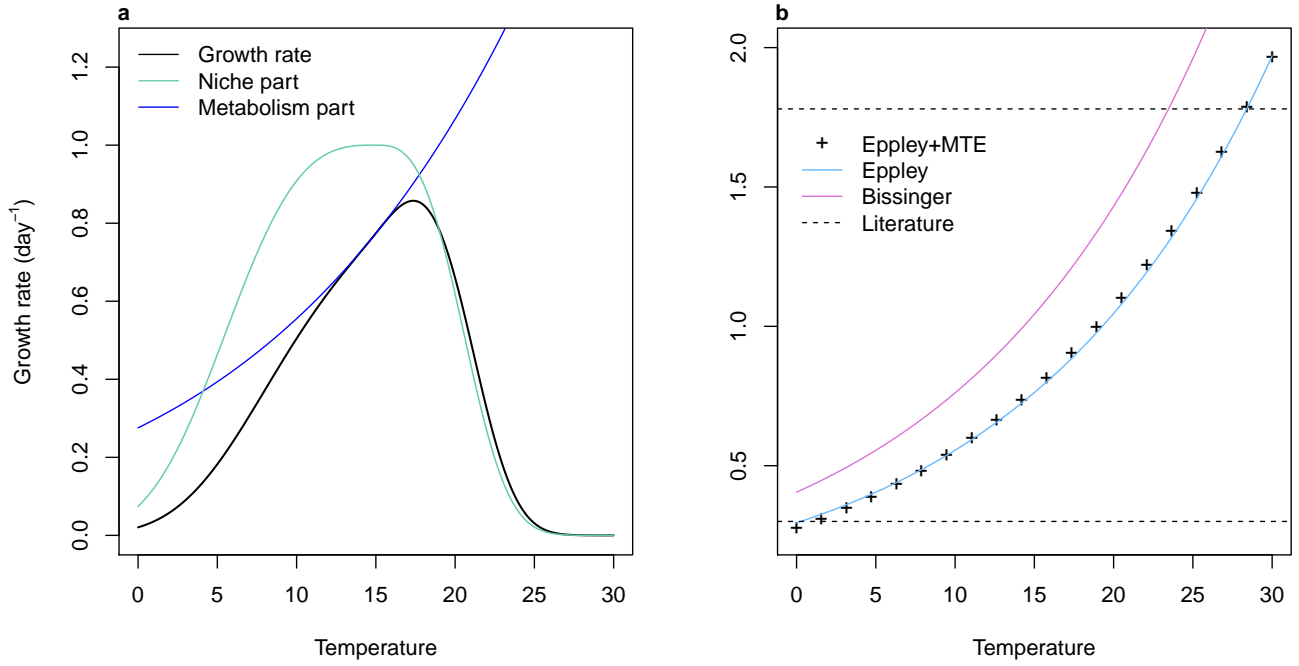


Figure S1: Decomposition of the Scranton & Vasseur (2016) growth rate formula (a). The black line indicates the final growth rate with their model. The blue line corresponds to the species-specific response to temperature for a thermal optimum of 15°C and the green line is the maximum achievable growth rate, a composite of the metabolic theory of ecology and the formula by Eppley (1972). This formula is shown by black crosses in (b) and compared to the Eppley (1972) curve in blue and Bissinger *et al.* (2008) formula in purple. Horizontal lines show limits found in the literature (Reynolds, 2006).

Species-specific response to temperature

The niche part of the growth rate $f_i(T)$ is mainly defined by two parameters which drive the phenology of a species: the thermal optimum T_i^{opt} and a proxy of the niche width b_i (eq. 2).

$$f_i(T) = \begin{cases} \exp(-|T - T_i^{opt}|^3/b_i), & T \leq T_i^{opt} \\ \exp(-5|T - T_i^{opt}|^3/b_i), & T > T_i^{opt} \end{cases} \quad (2)$$

The annual dynamics of phytoplanktonic organisms is usually characterized by a blooming period and a lower concentration during the rest of the year. The bloom can be triggered by a combination of nutrient and light input, as well as a sufficient temperature. All parameters being more or less correlated to the seasonal rythm, it is reasonable to restrain this study to the effect of one variable, temperature.

We base our estimates of T_i^{opt} and b_i on field observations. For each taxon and each year, we define the beginning of the bloom as the date when the taxon abundance exceeds its median abundance over the year. The duration of the bloom is the number of days between the beginning and the date where abundance falls below the median value. Taxa are then separated into two groups. In the field, generalists are characterized by one long bloom in the year or several blooms during which the abundances oscillate around their median. Specialists tend to appear only once or twice in the year for shorter amounts of time. A genus is therefore defined as a generalist if its cumulated bloom days over a year last more than the average duration of all blooms (137 days) for at least 15 years over the 20 years of the time series, and as a specialist if they fall below this threshold.

In the models, we assume that generalists have a niche width between 15 and 30°C and specialists, between 5 and 10°C. We assume that temperatures outside of this range lead to a growth rate at least 10 times inferior to the

growth rate obtained at their thermal optimum ($\exp(-|7.5|^3/b_i) = 0.1$ for a niche width of 15°C). This leads to values of b_i between 180 and 1500 for generalists, and 7 and 55 for specialists. A set of b values is drawn from a uniform distribution within these boundaries. Meanwhile, taxa are ordered as a function of the mean cumulated bloom length and larger niche values are attributed to longer mean bloom length, i.e. $\sum \bar{L}_{i,b} > \sum \bar{L}_{j,b} \Rightarrow b_i > b_j$ where \bar{L} is the mean over 20 years of the annual cumulated lengths of the bloom

The thermal optimum T_i^{opt} was first defined as the mean minimum temperature of the bloom throughout the whole time series. However, this value led to blooms occurring mainly in the winter and needed to be increased by 5°C in order to simulate realistic phytoplankton cycles.

It should be noted that a variation in niche width also affects the final shape of thermal preferences. Indeed, when b_i increases, the niche term f_i has smaller variation in values around the thermal optimum. In this case, the final value of the growth rate is driven by the metabolism part of the equation (Fig. S2).

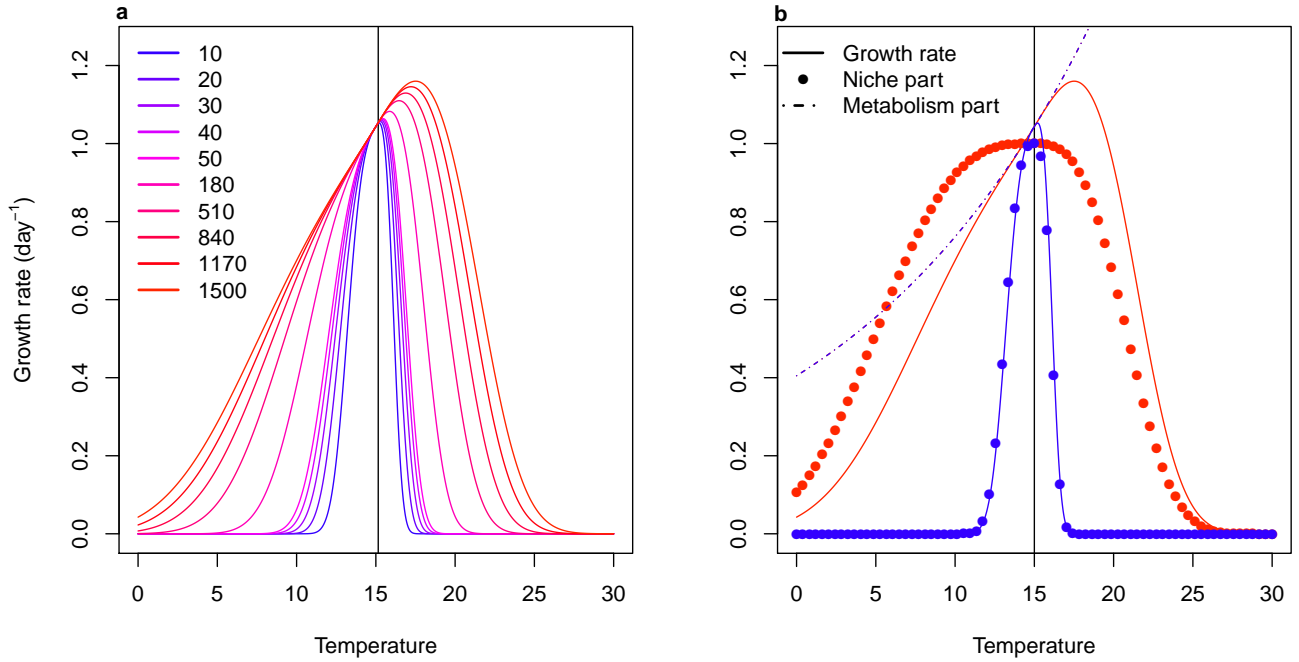


Figure S2: Relationship between daily growth rates and temperature with different values of niche width b (whose values are indicated in the legend, corresponding to specialist and generalist species) and the same thermal optimum, 15°C , indicated by the solid black line (a). On the right panel, only the two extreme values of b (10 and 1500) are shown in blue and red respectively. Solid lines then correspond to the final growth rate, points correspond to $f_i(T)$ values (see eq. 1) and the dotted line corresponds to $E(T)$ values.

We provide actual shapes of $f_i(T)$ for modeled taxa below (Fig S3).

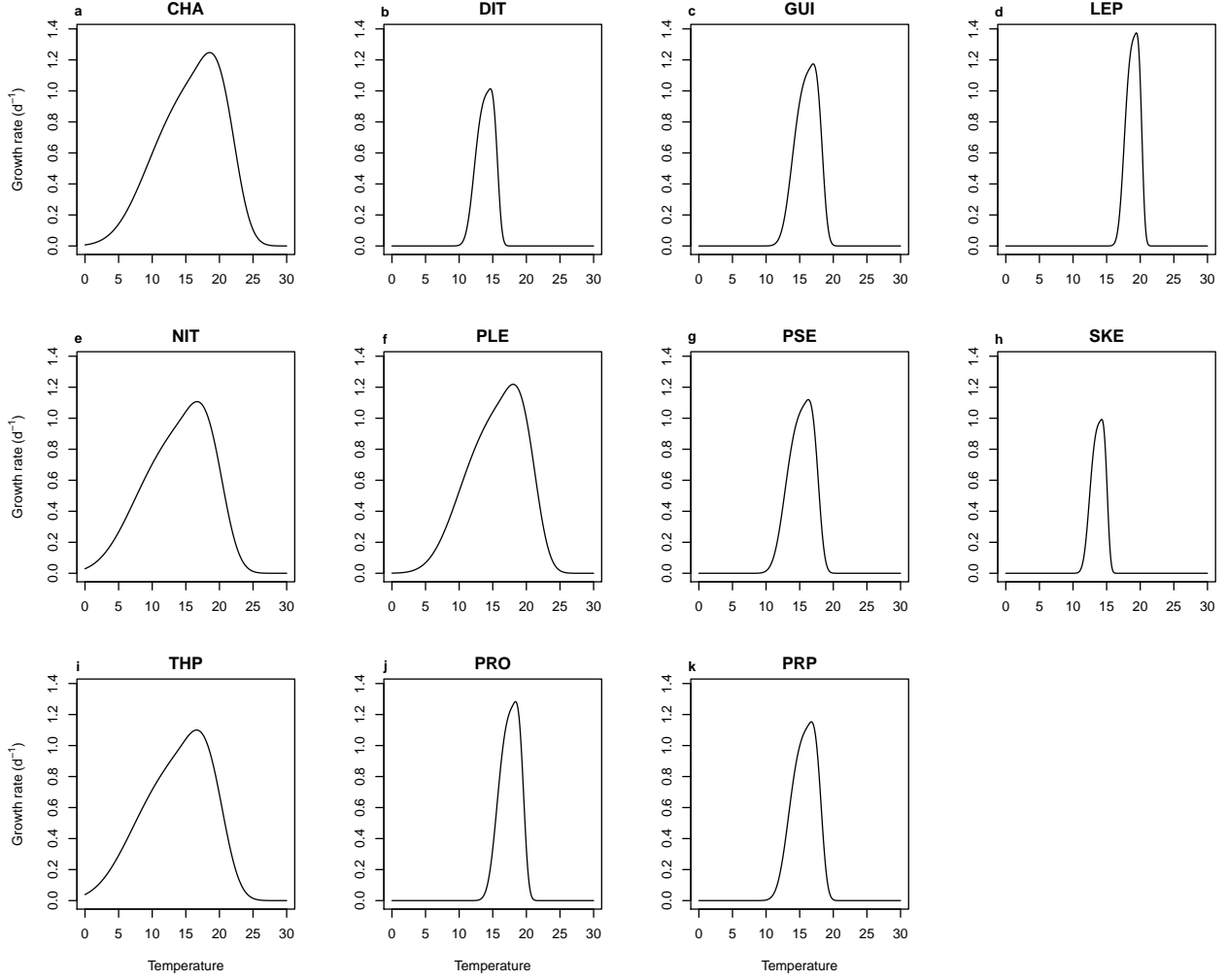


Figure S3: Growth rate as a function of temperature for the taxa used in the model (names are defined in Table 1).

S2 Initial estimates of interaction values

Model I: Lotka-Volterra interactions

Interactions between taxa have previously been computed with a Multivariate AutoRegressive model (eq. 3, Picoche & Barraquand, 2020).

$$\mathbf{n}_{t+1} = \mathbf{B}\mathbf{n}_t + \mathbf{C}\mathbf{u}_{t+1} + \mathbf{e}_t, \mathbf{e}_t \sim \mathcal{N}_S(0, \mathbf{Q}) \quad (3)$$

where S is the number of taxa, \mathbf{n}_t is the $1 \times S$ vector of log-abundance of phytoplankton taxa, \mathbf{B} is the $S \times S$ interaction matrix with elements b_{ij} (the effect of taxon j on taxon i), \mathbf{C} is the $S \times V$ environment matrix describing the effects of variables \mathbf{u}_{t+1} on growth rates and the noise \mathbf{e}_t is a $1 \times S$ noise vector following a multivariate normal distribution with a variance-covariance matrix \mathbf{Q} . The interaction model we use in the present paper is a Beverton-Holt multispecies model (eq. 1), also called at times Leslie-Gower. In Picoche & Barraquand (2020)'s Supporting information, we showed that MAR and BH interaction coefficients, respectively b_{ij} and α_{ij} , could map once abundances at equilibrium N_i^* are defined.

$$\begin{cases} b_{ii} - 1 = \frac{-\alpha_{ii}N_i^*}{1+\sum_l \alpha_{il}N_l^*} \\ b_{ij, i \neq j} = \frac{-\alpha_{ij}N_j^*}{1+\sum_l \alpha_{il}N_l^*} \end{cases}$$

Let's define \tilde{b}_{ij} with $\tilde{b}_{ii} = b_{ii} - 1$, and $f_A(i) = \sum_l \alpha_{il}N_l^*$.

$$\tilde{b}_{ij}(1 + f_A(i)) = -\alpha_{ij}N_j^*$$

We then sum on columns (on j).

$$\begin{aligned} \sum_j [\tilde{b}_{ij}(1 + f_A(i))] &= -f_A(i) \\ \Leftrightarrow -f_A(i)(1 + \sum_j \tilde{b}_{ij}) &= \sum_j \tilde{b}_{ij} \\ \Leftrightarrow f_A(i) &= -\frac{\sum_j \tilde{b}_{ij}}{(1 + \sum_j \tilde{b}_{ij})} \\ \Leftrightarrow \alpha_{ij} &= -\frac{1}{N_j^*} \tilde{b}_{ij} \left(1 - \frac{\sum_j \tilde{b}_{ij}}{1 + \sum_j \tilde{b}_{ij}}\right) \\ \Leftrightarrow \alpha_{ij} &= -\frac{1}{N_j^*} \frac{\tilde{b}_{ij}}{1 + \sum_j \tilde{b}_{ij}} \end{aligned}$$

This gives an exact correspondence between α_{ij} and b_{ij} . In the multispecies BH model, the presence of mutualistic interactions can lead to an orgy of mutual benefaction (May, 1981). We impose a minimum value of 1 to the denominator of the BH formulation, meaning that the growth rate cannot be higher than the maximum growth rate calculated, $r_i(T)$. We acknowledge the possibility of overyielding, i.e. an increase in biomass due to the presence of other species, but the phenomenon seems quite rare for phytoplanktonic communities (see Schmidtke *et al.* 2010 for underyielding and see Shurin *et al.* 2014 for an observed but not frequent, and small, overyielding).

Model II: saturating interactions

We now move to a model with saturating interactions between taxa.

$$N_{t+1,i} = \frac{e^{r_i(T)} N_{t,i}}{1 + \sum_{j/a \in \mathbb{C}} \frac{a_C N_{t,j}}{H_{ij} + N_{t,j}} + \sum_{j/a \in \mathbb{F}} \frac{a_F N_{t,j}}{H_{ij} + N_{t,j}}} \quad (4)$$

where coefficients a_C and a_F are the maximum interaction strength for competition and facilitation respectively, H_{ij} is the abundance of taxon j to reach half of the maximum effect of taxon j on taxon i , and \mathbb{C} and \mathbb{F} are the sets of competitive and facilitative interactions. This formula can be linked to the Unique Interaction Model by Qian & Akçay (2020), i.e. each taxon provides a unique type of benefit or disadvantage to the focus taxon.

There is no single solution for matching the \mathbf{B} matrix of the MAR model and model II including H_{ij} , a_C and a_F . We approximate the maximum interaction strength a_C as the average sum of all taxon effects $\alpha_{ij}N_j$ exerted on a given taxon if all interactions were competitive (eq. 5). To compute a_F , we can make two assumptions: on average, a) there is 70% facilitation in our dataset and b) the growth rate $r_i(T)$ should not exceed 1, as in model I. We

consider that the relationships that apply to individual interactions α_{ij} should also apply to the saturation point (eq. 6).

$$a_C = \frac{1}{S} \sum_i \left(\sum_j \alpha_{ij} N_{j,max} \right) \quad (5)$$

$$(1 - 0.7)a_C + 0.7a_F = 0 \quad (6)$$

At low abundances, we can consider that interactions are far from saturation. Taking the tangent of the function at this point, H_{ij} can be approximated by $f \frac{a_C/F}{\alpha_{ij}}$, where $f = 2$ is a correction factor that takes into account the fact that the slope at origin for the type II response is likely higher than the slope for a linear effect of density.

S3 Choice of parameters derived from literature

This section contains additional information on “fixed” parameters definitions and chosen values. Note that these values are then subjected to sensitivity analysis.

Loss rate The loss rate corresponds to multiple mortality processes. The Lotka-Volterra model of Scranton & Vasseur (2016) considered a rate around 0.04 day^{-1} . In Jewson *et al.* (1981), washout (0.5%), parasitism (4% of cells are infested and die) and grazing still remained low (about 0.05%) when compared to growth rates. Li *et al.* (2000) found values between 0.02 and 0.1 day^{-1} for natural mortality only, while a review by Sarthou *et al.* (2005) indicated a loss of daily primary productivity around 45% due to grazing only, 0.13 day^{-1} being potentially due to cell autolysis (in the absence of nutrients, or because of viral charge). Trying to make a compromise emerge from the literature above, we set the reference value to 0.2 day^{-1} .

Sinking rate Among the hydrodynamics processes that drive the sinking rate, turbulence and eddies – themselves driven by tidal currents, the shape of the coast or wind conditions – are influential in keeping the cells at the top of the water column. For that reason, laboratory experiments on sinking rates are not sufficient to calibrate a field-based model. We therefore chose sinking rate values from field studies. In the Gotland Basin (central Baltic Sea), Passow (1991) measured a large variability in sinking rates, even within the same genus (e.g., between 1 and 30% for *Chaetoceros* spp.). However, a pattern could be highlighted, with a small number of genera that sank more than the rest of the community. The mean sinking rate for *Chaetoceros* and *Thalassiosira* was around 10% while it was around 1% for the other species. Sinking rate values around 10% are consistent with the loss rates in Kowe *et al.* (1998) in a river and Wiedmann *et al.* (2016) in an estuary (mouth of Adventfjorden). When estimating changes of the sinking rate over time, values between 4 and 50% were obtained (Jewson *et al.*, 1981). We therefore chose to represent the sinking rates with a Beta-distribution (Fig. SS4) which accounts for observed maximum and mean values, while still allowing a highly skewed distribution of sinking rates between species. High sinking rates are attributed to the morphotypes corresponding to *Chaetoceros* (CHA) and *Thalassiosira* (THP).

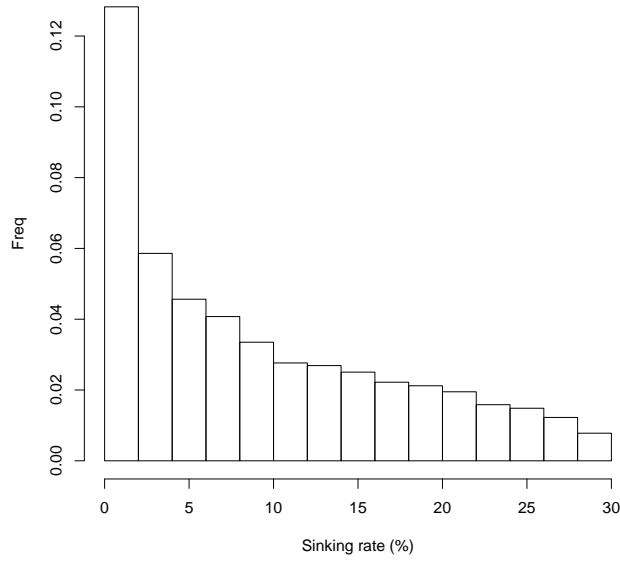


Figure S4: Possible Beta-distribution of sinking rates

Cyst mortality and burial McQuoid *et al.* (2002) present maximum and mean depth of sediment at which germination of diatoms and dinoflagellates could still occur when incubated. The authors also present sediment datation according to depth. Depth can therefore be related to maximum and mean age of phytoplankton cysts before death. Assuming m is the probability of mortality and the survival follows a geometric law, the life expectancy of a cyst is $\frac{1}{m} \Leftrightarrow m = \frac{1}{L_{mean}}$ where L_{mean} is the average duration of cyst viability. Another way to look at the process is that life expectancy L follows the distribution $p(L > l) = e^{-ml}$. We can arbitrarily choose that for the older cysts (i.e., the ones buried the deepest), $p(L > l_{max}) = 0.05$. In this, $m = -\frac{\ln(p(L > l_{max}))}{l_{max}}$. In both cases, m varies between 10^{-5} day^{-1} and 10^{-4} day^{-1} .

As we highlight in the main text, burial is a very important process that controls the availability of cysts, conditional to their survival in the sediment. However, burial rate is almost entirely dependent on the local sedimentation and no generally applicable literature could be found. We varied it between 0.001 and 0.1 per day.

Resuspension As mentioned in the main text, resuspension values are mostly taken from models or data for inorganic particles. Rates vary greatly from one publication to another: in Fransz & Verhagen (1985), in a coastal area, the resuspension rate of sediments is evaluated around $5 \times 10^{-5} \text{ day}^{-1}$ in winter and decreases in summer, with a relationship between resuspension and the light extinction coefficient. In Kowe *et al.* (1998), the resuspension rate of diatoms is evaluated around $1.9 \times 10^{-5} \text{ day}^{-1}$. In Le Pape *et al.* (1999), resuspension rate of sediments and dead diatoms is 0.002 day^{-1} . In this paper, we explore values between 10^{-5} (stratified water column) to 0.1 (highly mixed environment).

Finally, it should be noted that cyst burial, sinking rate and resuspension are all highly contingent upon the local hydrodynamics and therefore are intermingled processes.

S4 Phytoplankton taxa at the calibration site

Code	Taxa
CHA	<i>Chaetoceros</i>
DIT	<i>Ditylum</i>
GUI	<i>Guinardia</i>
LEP	<i>Leptocylindrus</i>
NIT	<i>Nitzschia+Hantzschia</i>
PLE	<i>Pleurosigma+Gyrosigma</i>
PRO	<i>Prorocentrum</i>
PRP	<i>Protoperidinium+Archaeperidinium+Peridinium</i>
PSE	<i>Pseudo-nitzschia</i>
SKE	<i>Skeletonema</i>
THP	<i>Thalassiosira+Porosira</i>

Table 1: Name and composition of the phytoplanktonic groups used in main text, see Picoche & Barraquand (2020) for more information on these taxa.

S5 Phytoplankton time series with model II

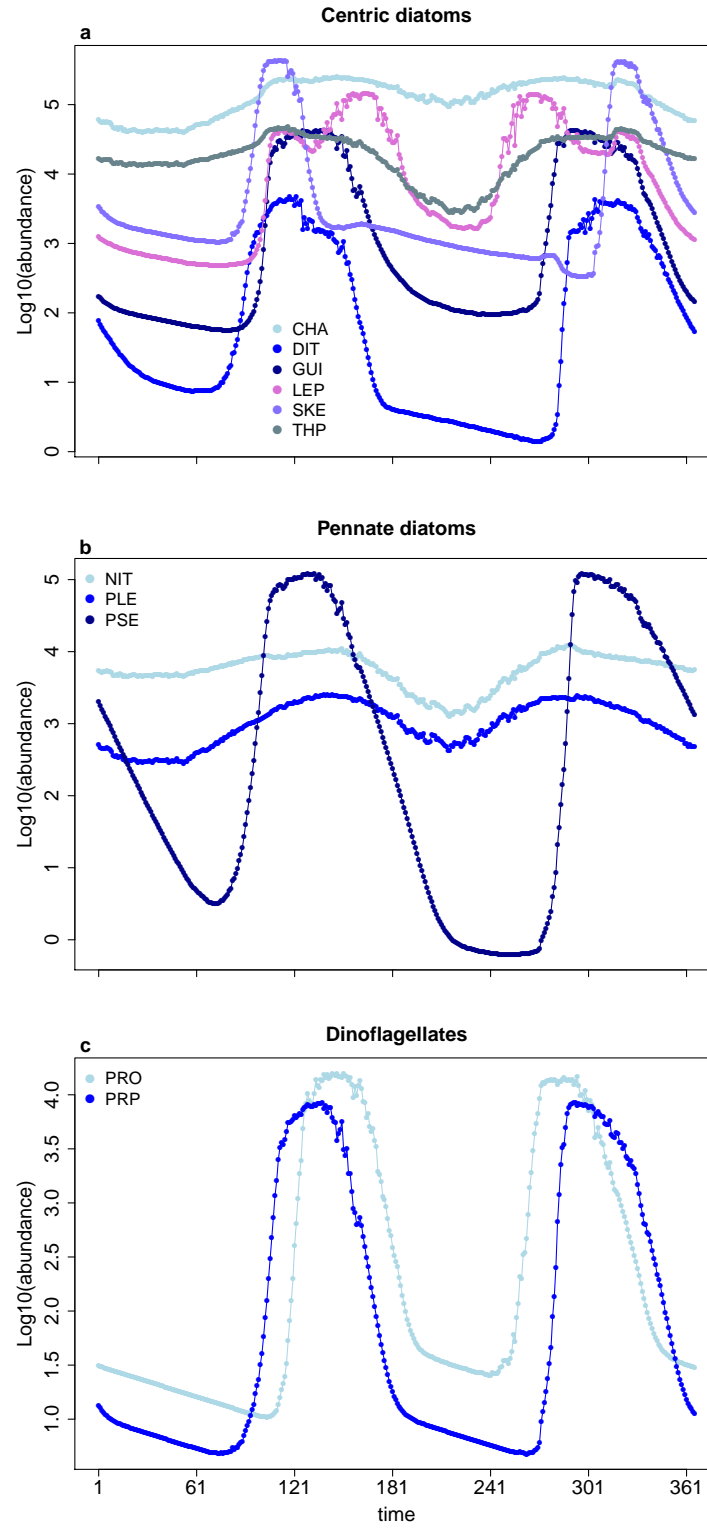


Figure S5: Simulated phytoplankton time series for a year in model II (with saturating interactions). Each panel corresponds to a cluster of interacting taxa.

S6 Scenario: changing interspecific interaction strengths but not intraspecific interaction strengths

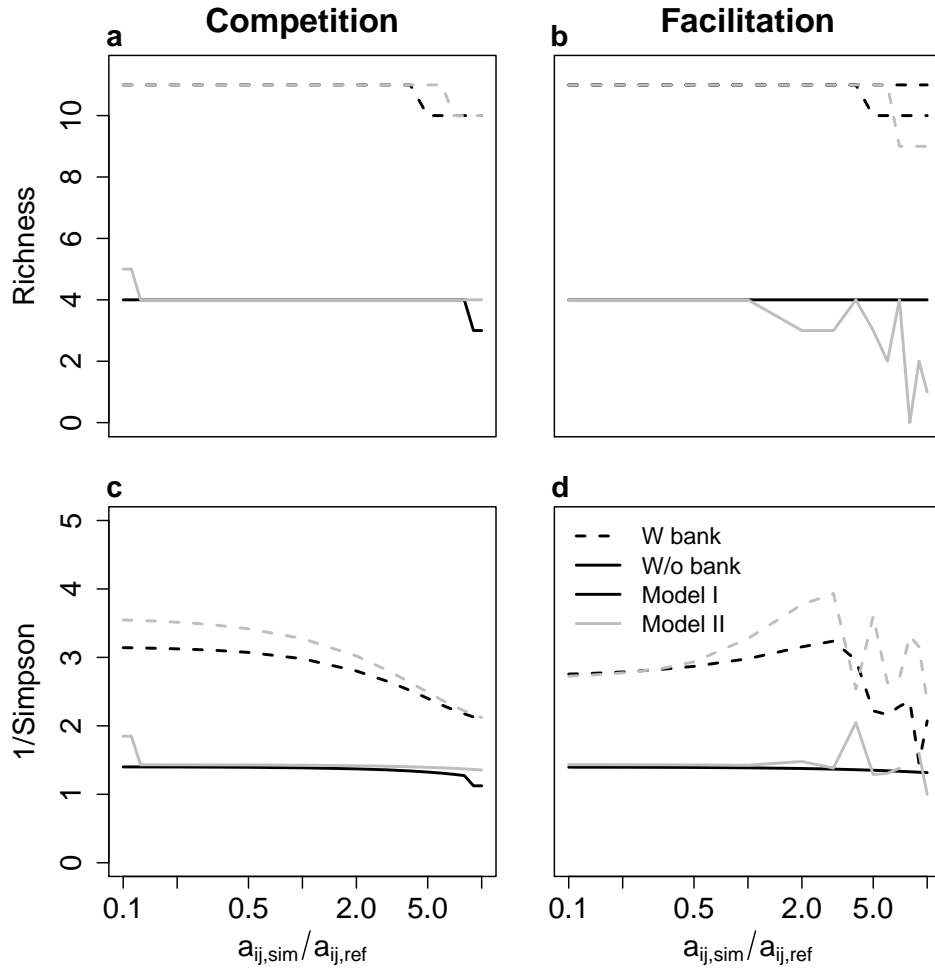


Figure S6: Measures of biodiversity in the ocean at the end of the simulation: a-b) richness and c-d) inverse of the Simpson index, with (dashed line) and without (solid line) a cyst bank, as a function of the strength of competition and facilitation with a classical Beverton-Holt (black lines) or a saturating interaction (grey lines) formulation, keeping the same values for the intraspecific interaction strengths. The x-axis shows the factor by which each interaction coefficient was multiplied (note the logarithmic scale)

When intraspecific interaction strengths do not change, reducing the values of interspecific competition has very little effect on both richness and the inverse of the Simpson index. Increasing facilitation finally destabilizes the ratio of intra- to interspecific interaction strengths, which destabilizes the community and leads to the observed diversity decrease in the absence of a cyst bank.

S7 Growth rates and survival without a cyst bank

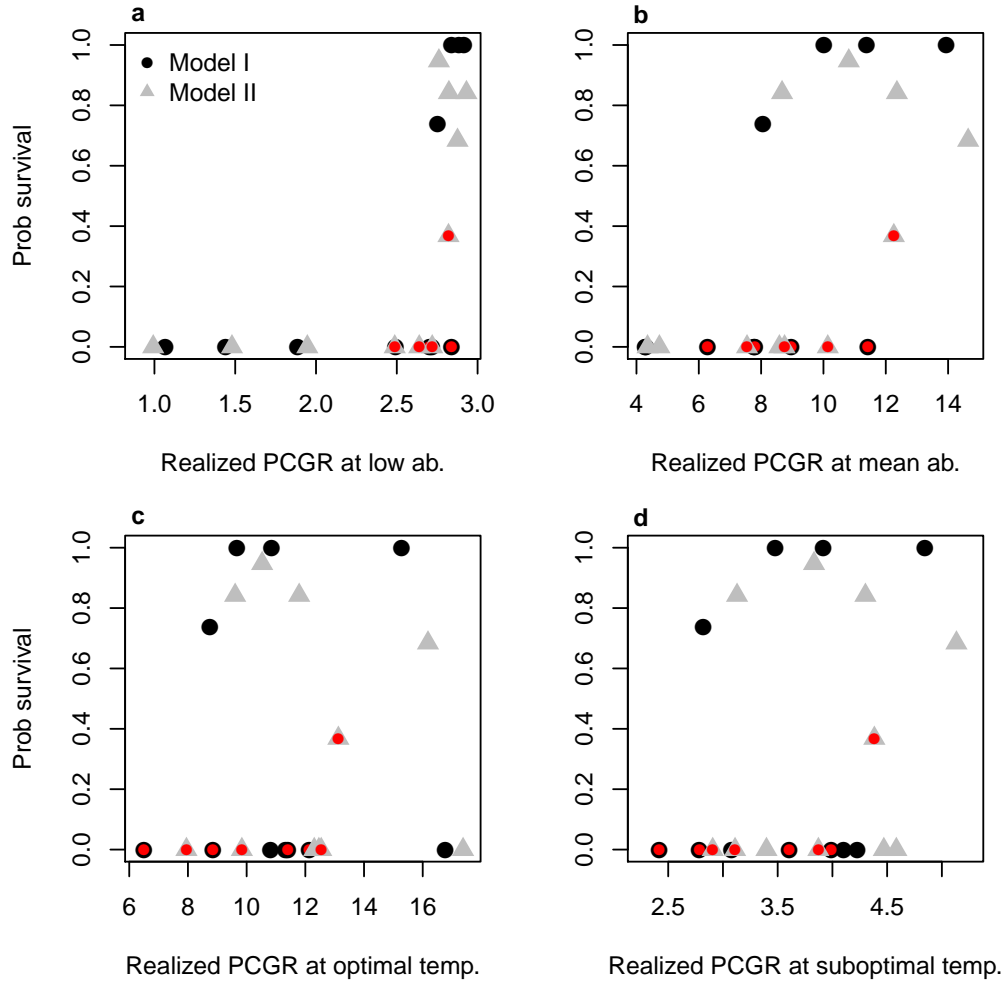


Figure S7: Probability of survival in the absence of a cyst bank as a function of the realized per capita growth rates (PCGR) of each species in different conditions. We consider mean temperature and low densities (a), i.e., all species density are 1 C/L, or average densities (b), i.e., all species are at their simulated average density values; or average densities and optimal temperature for each species (c), or suboptimal temperatures (d) - here, 30°C. Red points correspond to species which have a high growth rate at low density but still goes extinct.

Extinction in the absence of the cyst bank can be explained by both a low growth rate at low density and average temperature (affecting specialists with a narrow niche) and a low growth rate at average density despite being at optimal temperature (i.e., species strongly affected by interactions).

References

Bissinger, J., Montagnes, D., Harples, J. & Atkinson, D. (2008). Predicting marine phytoplankton maximum growth rates from temperature: Improving on the Eppley curve using quantile regression. *Limnology and Oceanography*, 53, 487–493.

- Edwards, K., Thomas, M., Klausmeier, C. & Litchman, E. (2015). Light and growth in marine phytoplankton: allometric, taxonomic, and environmental variation. *Limnology and Oceanography*, 60, 540–552.
- Edwards, K., Thomas, M., Klausmeier, C. & Litchman, E. (2016). Phytoplankton growth and the interaction of light and temperature: A synthesis at the species and community level. *Limnology and Oceanography*, 61, 1232–1244.
- Eppley, R. (1972). Temperature and phytoplankton growth in the sea. *Fishery Bulletin*, 70, 1063–1085.
- Fransz, H. & Verhagen, J. (1985). Modelling research on the production cycle of phytoplankton in the Southern Bight of the North Sea in relation to riverborne nutrient loads. *Netherlands Journal of Sea Research*, 19, 241–250.
- Jewson, D.H., Rippey, B.H. & Gilmore, W.K. (1981). Loss rates from sedimentation, parasitism, and grazing during the growth, nutrient limitation, and dormancy of a diatom crop. *Limnology and Oceanography*, 26, 1045–1056.
- Kowe, R., Skidmore, R., Whitton, B. & Pinder, A. (1998). Modelling phytoplankton dynamics in the River Swale, an upland river in NE England. *Science of The Total Environment*, 210, 535–546.
- Le Pape, O., Jean, F. & Ménesguen, A. (1999). Pelagic and benthic trophic chain coupling in a semi-enclosed coastal system, the Bay of Brest (France): a modelling approach. *Marine Ecology Progress Series*, 189, 135–147.
- Li, M., Gargett, A. & Denman, K. (2000). What determines seasonal and interannual variability of phytoplankton and zooplankton in strongly estuarine systems? *Estuarine, Coastal and Shelf Science*, 50, 467–488.
- May, R.M. (1981). *Theoretical Ecology: Principles and Applications*. Oxford University Press UK.
- McQuoid, M.R., Godhe, A. & Nordberg, K. (2002). Viability of phytoplankton resting stages in the sediments of a coastal Swedish fjord. *European Journal Phycology*, 37, 191–201.
- Passow, U. (1991). Species-specific sedimentation and sinking velocities of diatoms. *Marine Biology*, 108, 449–455.
- Picoche, C. & Barraquand, F. (2020). Strong self-regulation and widespread facilitative interactions between genera of phytoplankton. *Journal of Ecology*.
- Qian, J. & Akçay, E. (2020). The balance of interaction types determines the assembly and stability of ecological communities. *Nature Ecology & Evolution*, 4, 356–365.
- Reynolds, C.S. (2006). *The ecology of phytoplankton*. Cambridge University Press.
- Sarthou, G., Timmermans, K.R., Blain, S. & Tréguer, P. (2005). Growth physiology and fate of diatoms in the ocean: a review. *Journal of Sea Research*, 53, 25–42.
- Schmidtke, A., Gaedke, U. & Weithoff, G. (2010). A mechanistic basis for underyielding in phytoplankton communities. *Ecology*, 91, 212–221.
- Scranton, K. & Vasseur, D.A. (2016). Coexistence and emergent neutrality generate synchrony among competitors in fluctuating environments. *Theoretical Ecology*, 9, 353–363.
- Shurin, J.B., Mandal, S. & Abbott, R.L. (2014). Trait diversity enhances yield in algal biofuel assemblages. *Journal of Applied Ecology*, 51, 603–611.
- Wiedmann, I., Reigstad, M., Marquardt, M., Vader, A. & Gabrielsen, T. (2016). Seasonality of vertical flux and sinking particle characteristics in an ice-free high arctic fjord-Different from subarctic fjords? *Journal of Marine Systems*, 154, 192–205.